

Ying-Khai Teh and Philip K.T. Mok

This chapter complements other chapters on battery technologies and on-chip DC-DC conversion, and mainly addresses the challenges of designing low power IoT nodes that are powered by energy harvesting sources, which is the key enabling technology to extend battery life and minimize manual battery maintenance, using *in situ* power extraction from the surrounding. Energy harvesting options, circuit concepts, considerations and trade-offs regarding circuit topology, passive component and CMOS process are surveyed. In particular, recent circuit solutions involving non-conventional power management schemes specifically catering for energy-harvesting-assisted IoT systems will be discussed and compared.

Y.-K. Teh
Hong Kong University of Science and Technology,
Clear Water Bay, Hong Kong

San Diego State University, San Diego, CA, USA

P.K.T. Mok (✉)
Hong Kong University of Science and Technology,
Clear Water Bay, Hong Kong
e-mail: eemok@ust.hk

11.1 Available Energy Sources for IoT

11.1.1 Classification of Energy Source Characteristics and Classification

Advancement in the thin-film fabrication has successfully produced new generation of energy harvesters at reasonable cost, comes with compact size and able to generate microwatts range of power via surrounding events. An overview of energy harvesters commercially available are given in this section, which include thermoelectric generator (TEG), microbial fuel cell (MFC), photovoltaic cell (PVC) and piezoelectric harvester (PEH). Key classification matrix to characterize the energy sources are defined and outlined, i.e. power profile (current-voltage) and availability (continuous-time, discrete-time), and physical profile. Energy sources which are highly volatile in nature (photovoltaic cell (PVC) in rough, cloudy environment or piezoelectric harvester (PEH) installed in poor vibration frequency band) are considered as discrete-time (DT) energy source; which have high output voltage once ready, but suffers intermittency in term of power availability.

Energy sources such as body-powered TEG and MFC are considered as continuous-time (CT) energy source (Bandyopadhyay and Chandrakasan 2012; Danesh and Long 2011).

Although the output voltage is low (<300 mV), the available energy is stable and omnipresence.

Table 11.1 classifies these four energy harvesters into according to voltage-current-time matrix. Table 11.2 summarizes key device characteristics of four different energy harvesters under low output power condition (less than $100 \mu\text{W}$) i.e. TEG only has 2°C of temperature difference between the Peltier junctions, MFC with 50 ml of biofuel, PVC is illuminated at 200 lux (indoor lighting condition) and PEH is vibrated at 0.1 g. Figure 11.1 shows the power density of different energy sources, assuming all are at maximum power point. TEG which has the best power density performance has attracted the most research attentions in recent decade.

11.1.2 Continuous-Time Energy Sources (TEG and MFC)

TEG is an interesting energy harvester for its continuous operation against environmental condition change, due to omnipresence of thermal energy gradient (which manifests as temperature

difference). State-of-the-art TEGs are fabricated using thin-film deposition technology of Bi_2Te_3 material. Such improvements are desirable for further system miniaturization. The new generation TEG (**Micropelt**) has smaller device area with increased power density ($100 \mu\text{W}/\text{mm}^2$), compared to conventional bulk material based TEGs (**Marlow Industries**) ($13 \mu\text{W}/\text{mm}^2$) at temperature difference of 10°C . Internal resistance (R_{TEG}) of new generation TEG is 400Ω , which is 80 times larger whereas the absolute output power for conventional TEG is 8 times higher. The output power and power density comparisons of the two TEGs are shown in Fig. 11.2. Simplified circuit model of TEG (**Micropelt**), and its current-voltage characteristics are shown in Fig. 11.3.

Besides thermoelectric solution, another emerging power source is microbial fuel cells (MFC). MFC harvests electricity from organic dispose such as waste water, which is essentially by-product of catalytic activities of microorganisms over various organic substrates. The nature where MFC derives its energy enables the niche application of waste water treatment and water quality monitor systems.

Table 11.1 Classifications of energy sources

Type	TEG (Micropelt)	MFC Wang et al. (2013)	PVC (Enocean)	PEH (Microgen)
Voltage	Low	Low	High	High
Current	High	High	Low	Low
Time	CT	CT	DT	DT

CT, continuous time; DT, discrete time

Table 11.2 Device characteristics of energy sources

Type	TEG (Micropelt)	MFC Wang et al. (2013)	PVC (Enocean)	PEH (Microgen)
V_{OC} (max)	0.3 V	0.6 V	4 V	8 V (rectified)
I_{SC} (max)	$750 \mu\text{A}$ (@ $\Delta T = 2^\circ\text{C}$)	2.7 mA	$7 \mu\text{A}$ (@200 lux)	$14 \mu\text{A}$ (@0.1 g)
$V_{\text{MPP}}^{\text{a}}$	0.15 V (@ $\Delta T = 2^\circ\text{C}$)	0.35 V	3 V (@200 lux)	4 V (@0.1 g)
$P_{\text{MPP}}^{\text{b}}$	$56 \mu\text{W}$ (@ $\Delta T = 2^\circ\text{C}$)	$440 \mu\text{W}$	$14 \mu\text{W}$ (@200 lux)	$56 \mu\text{W}$ (@0.1 g)
Dimension (L \times W \times H mm ³)	$4 \times 3 \times 1$	$37 \times 37 \times 37$	$35 \times 13 \times 1$	$15 \times 15 \times 6$
Power density ($\mu\text{W}/\text{mm}^3$)	4.67	8.68×10^{-3}	0.03	0.04

^a V_{MPP} = Operating voltage of energy source at maximum power point

^b P_{MPP} = Output power of energy source at maximum power point

Current state-of-the-art MFCs are fabricated using emerging material such as graphene (Wang et al. 2013). It is interesting to note that thin-film TEG operating at low temperature difference (4–5 °C) and graphene-based MFC have similar electrical characteristics, as shown in Fig. 11.4. Nonetheless MFC’s power density is approximately three orders lower than TEG’s. Electrically both energy sources can be modeled as an ideal voltage source (V_{GEN}) in series with internal resistance (R_S) of a few hundred ohms.

11.1.3 Discrete-Time Energy Sources (PVC and PEH)

Photovoltaic cell (PVC) is capable of converting light directly into electric energy. Most PVCs consist of silicon material. Due to the high cost of the vacuum-based fabrication process of such solar cells, research and development has been directed toward the invention and development of thin film inorganic and emerging inorganic/organic thin film PV solar cells in an attempt to fabricate solar cells out of less-expensive materials and processes. Light is often present for a prolonged period, during which the light energy can be accumulated in storage mechanisms and then used when needed. Simplified circuit model of PVC in (Enocean) and typical output behavior is shown in Fig. 11.5.

Piezoelectric harvester (PEH) with size smaller than a US quarter coin and internal parasitic capacitance of a few nano Farad can be manufactured via commercial CMOS process (Microgen). The generated power is in alternating current (AC) mode and thus requires to be rectified before use. Simplified circuit model of PEH with rectified output in (Microgen) and its typical output behavior is shown in Fig. 11.6. However, as miniaturization continues, the mechanical vibration bandwidth for smaller devices is also getting smaller (a few Hertz). Therefore PEH is sensitive

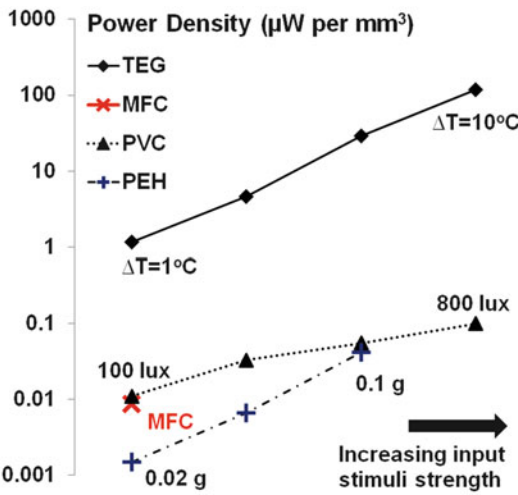


Fig. 11.1 Power density of TEG (Micropelt), MFC (Wang et al. 2013), PVC (Enocean) and PEH (Microgen)

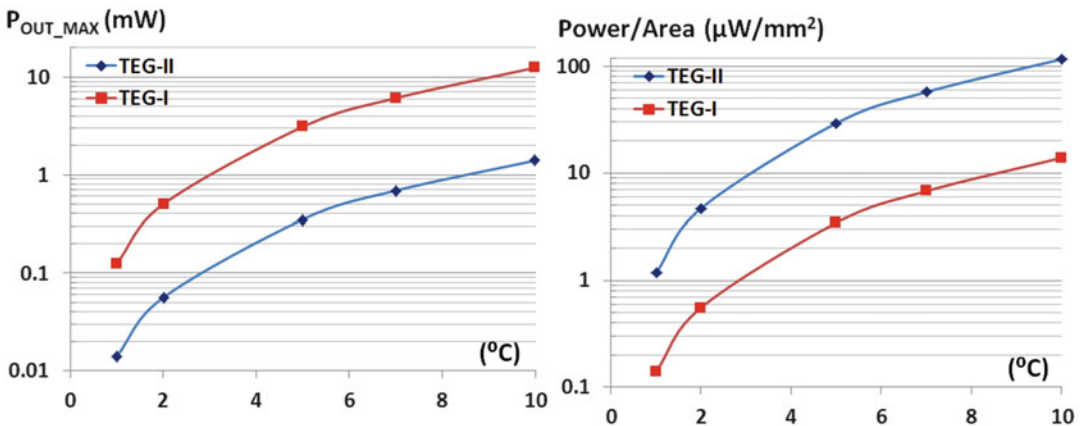


Fig. 11.2 Power and Power density of conventional TEG (TEG-I (Marlow Industries)) and new generation TEG (TEG-II (Micropelt))

Fig. 11.3 Simplified equivalent circuit model and output characteristics of TEG (MicroPelt)

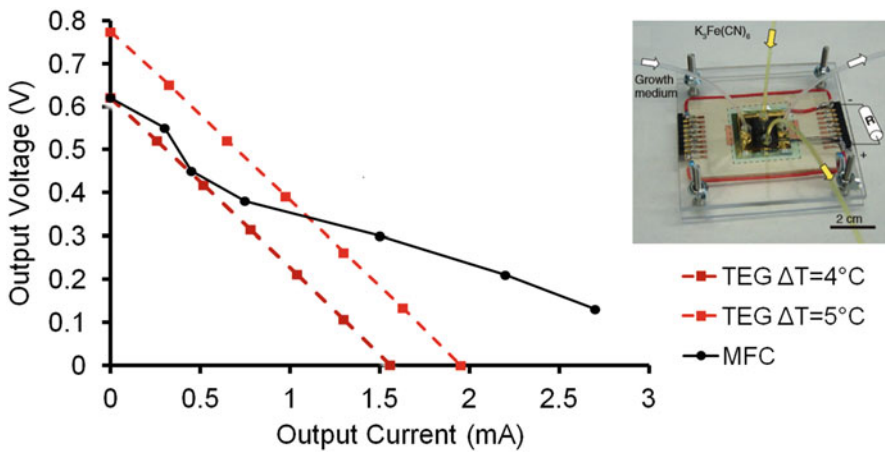
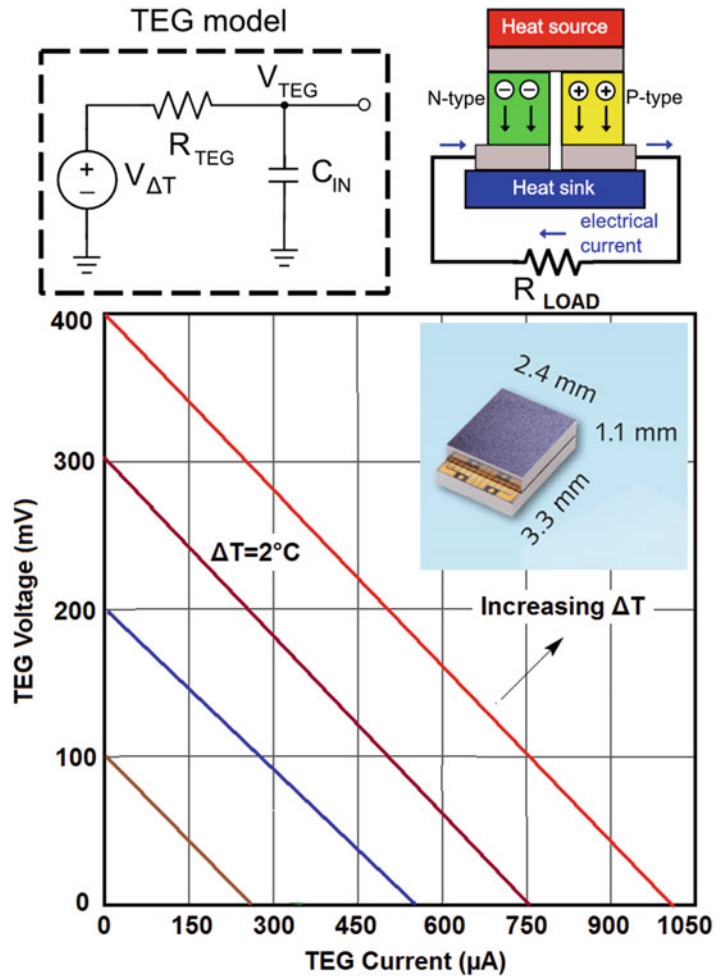


Fig. 11.4 I-V characteristics of TEG (MicroPelt) at $\Delta T = 4^\circ C$, $\Delta T = 5^\circ C$ and MFC (Wang et al. 2013)

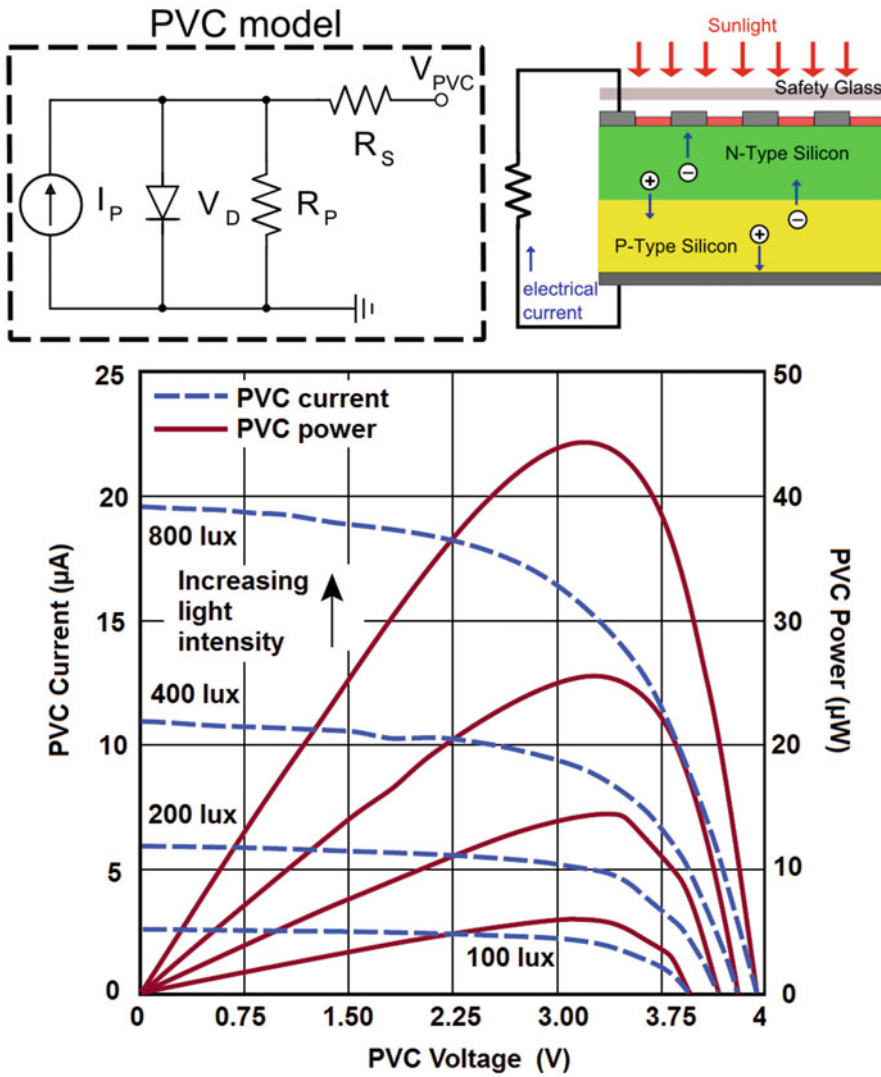


Fig. 11.5 Simplified equivalent circuit model of PVC and its output characteristics (Enocean)

towards environment stimuli and the output power profile is highly volatile.

11.2 Comparison of Battery-Powered and Energy-Harvested Systems

In this section, the difference of battery-powered and energy-harvested systems primarily lies on the known and unknown voltage-current profile, due to different source resistance is highlighted.

The fundamental difference between battery power source and energy harvesting source is that energy harvesters have significantly higher source resistance (much higher than 1Ω) compared to battery (less than 1Ω). However, in battery powered application, charge stored in non-rechargeable battery is limited. Before the battery stored charge depletes, power sourcing capability of a battery is much higher than energy harvesting source in general (Table 11.3).

For energy harvesting source, supply of electrical charge is in theory unlimited and most of

Fig. 11.6 Simplified equivalent circuit model of PEH and its output characteristics (Microgen)

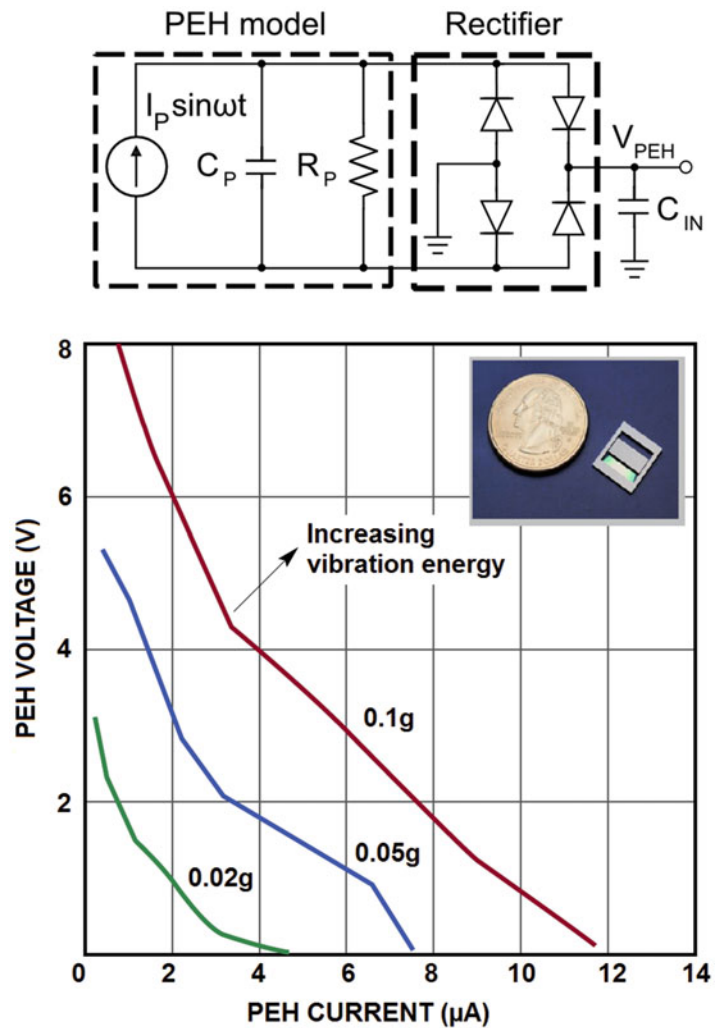


Table 11.3 Energy harvesting source vs. battery

Energy harvesting source	Battery
High internal resistance	Low internal resistance
Unlimited charge in theory	Finite charge
Limited instantaneous power (Duty cycled operation)	High instantaneous power (Duty cycled operation is optional)
DC-DC converter functions:	DC-DC converter functions:
– Output voltage regulation	– Output voltage regulation
– Maximum power point tracking (MPPT)	– No MPPT necessary

the time the energy harvester is charging up the storage capacitor. Before storage capacitor voltage reaches the designed threshold, the regulator is turned off. Having a shunt regulator in this scenario basically acts as charge release valve. The objective is to sense the storage capacitor voltage, once the set threshold is reached,

additional charge harvested will be dissipated by shunt regulator. If a series regulator is used instead, the system is prone to overvoltage failure as excess charge will continue to accumulate and build up storage capacitor voltage. Overvoltage protection should be prioritized over power conversion efficiency in this scenario. Hence the

automatic protection against overvoltage function of a shunt regulator is indeed attractive for energy harvesting application. High voltage headroom generated by PVC and PEH output can be absorbed by a properly designed shunt regulator such as (Sarkar and Chakrabarty 2013), allowing storage capacitor to be directly charged by these sources.

One key challenge is the design of interfacing power management circuit that efficiently combines many different sources of energy into one. Combining the power from variable sources conventionally requires a sophisticated control system as demonstrated in (Bandyopadhyay and Chandrakasan 2012). The control itself requires additional overhead power, i.e. first sense the availability of power from each source, then compute and optimize the multi-source time multiplexing.

Another challenge is the limit imposed by the low supply voltages in standard CMOS technologies. These constrain the output voltage to be within the defined supply voltage. At higher voltages outside of the nominal range, breakdown mechanisms and hot carrier effects will be present. Hence the power management circuit must prevent the overvoltage problem. On the other end of the spectrum, some energy sources have very low input voltage (<0.2 V), which are lower than transistor threshold voltage. At sub-threshold region, transistors are not fully turned on and conventional voltage converter topologies are no longer valid or suffer poor conversion efficiency.

Typical power consumption pattern of an IoT sensor node is low average power (no active power consumption except watch dog timer) but occasional occurrence of high concentrated burst of power to accomplish a task such as activating external sensors or sending radio packets. If these bursts occur with a low duty cycle such that the total energy needed for a burst can be accumulated between bursts then the output can be maintained entirely by the energy harvesters. An ideal energy harvesting scheme is required to maintain low leakage power of harvested energy during idle period yet able to supply high pulsed power on demand.

11.3 Energy Harvesting and Power Conditioning Circuits

Multi-level supply voltage (V_{DD}) is common for IoT systems implemented using low power modern CMOS process. External I/O interface circuits typically works at 3 V (5 V for legacy devices) and internal digital core circuits typically works at 1 V. Modules such as sensors, analog-to-digital-converters (ADC) and amplifiers always prefer higher voltage headroom to achieve better resolution, gain and linearity (Mak and Martins 2010). For battery-powered applications, such multiple output voltage can be realized using Single-Inductor-Multiple-Output (SIMO) DC-DC converter (Jing and Mok 2013; Ma et al. 2003a, b) or multiple series regulator i.e. low dropout regulator (LDO) (Ho and Mok 2012; Zhan and Ki 2012, 2014). The conventional approaches become unrealistic when the input power approaches microwatts range as the overhead power is too high to jeopardize the entire system operation. Design requirements of energy harvesting system to power a wireless sensor IoT node and the associated challenges hitherto discussed are summarized in Table 11.4.

In previous sections, electrical characteristics of various energy harvesting source and storage capacitors were reviewed. Based on these

Table 11.4 Summaries of design requirements and challenges of IOT wireless sensor node

Input voltage	0–8 V
Input current	0–1 mA
Input power	0–1 mW
Dual output voltage	1 V (Digital), 3 V (Analog, RF and sensors)
Design features required	<ul style="list-style-type: none"> – Smallest input voltage and power possible – Smallest overhead and leakage power possible – Highest voltage conversion ratio and efficiency possible – Self-start-up during cold-start state – Over-voltage protection – Maximum power point tracking

properties, this chapter surveys integral system schemes to accommodate multiple types of energy sources simultaneously and minimize storage leakage loss. Each circuit block that can be utilized to implement such systems i.e. linear regulator, switching and switched-capacitor DC-DC converters are stepped through briefly in sequential manner.

Different power converter control schemes will have different dynamic power loss. As rule of thumb, ZCS control is desired to maximize power efficiency. Pulse frequency modulation (PFM) has superior power efficiency than pulse-width modulation (PWM) schemes at light-load. Comparator is one of the most power-consuming circuit blocks in power converter. Designers should use low bias current or clocked comparator to save quiescent power. For energy harvesting source which is steady against environmental change, maximum power point tracking (MPPT) algorithm can be executed in a low duty cycle fashion to save computation power. For energy harvesting source with known, fixed source resistance, timing-based impedance matching MPPT technique can be employed with a comparator-less fully digital approach. This MPPT technique also avoids

interrupting energy harvesting flow since circuit does not need to pause and sample the energy harvester source open circuit voltage from time to time.

Table 11.5 summarizes the characteristics of different DC-DC converter circuits according to conversion possible, peak power efficiency and output voltage control that can be used to construct a multi-input-multi-output energy harvesting power management systems for IoT node.

11.3.1 Linear Regulator in Energy Harvesting Application

As discussed in Chap. 10, there are two possible implementations for linear regulators i.e. series and shunt regulators. In principle these circuits can be designed based on the functional blocks shown in Figs. 11.7 and 11.8 respectively by assuming the internal resistance of energy harvesting source to be series resistance R_S needed in any typical linear regulator realization. Series voltage regulator is more power efficient but lacks the ability to prevent over-voltage. Therefore if shunt regulator is used, constant

Table 11.5 Summary of different DC-DC converters

Type	Conversion direction (Up/Down)	Peak power efficiency	Output voltage
Linear regulator	Down	Low	Adjustable by reference voltage
Switching converter	Up/Down	High	Adjustable by clock duty cycle
Switched- capacitor	Up/Down	Medium	Adjustable by clock duty cycle

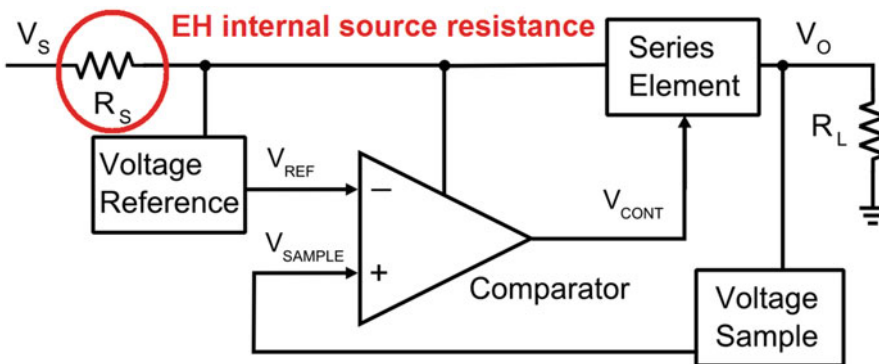


Fig. 11.7 Basic working principle of series voltage regulator

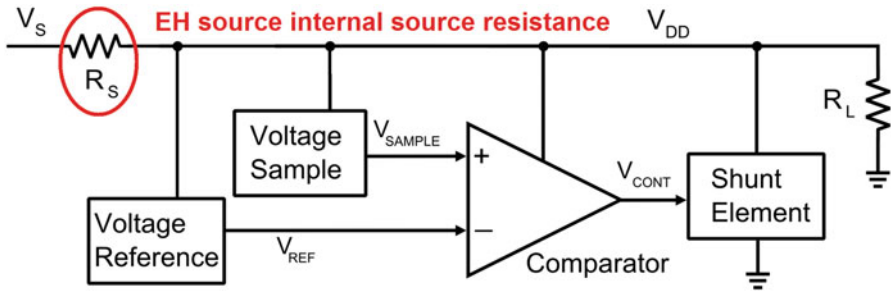
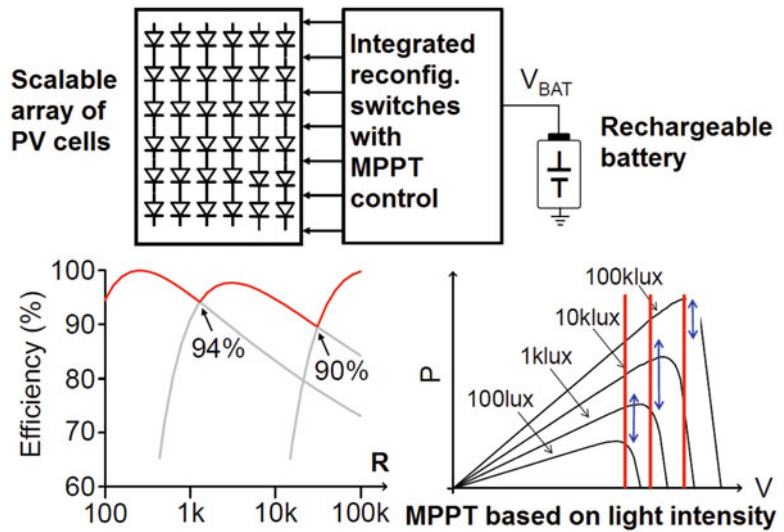


Fig. 11.8 Basic working principle of shunt voltage regulator

Fig. 11.9 Reconfigurable switch for photovoltaic energy harvesting



power will be drawn from battery despite the load power being low. This is disaster especially for low duty long working hour IoT application because battery charge depletes quickly. This scenario is exactly how the conventional wisdom i.e. series regulator is more efficient is being derived. Shunt voltage regulator is less power efficient but it can protect the circuit from over-voltage, which is useful when interfacing with high voltage low input energy source. However, linear regulator can only step down input voltage to generate a lower output voltage. The best conversion power efficiency possible is V_O/V_S , which implies that this type of regulator is considered efficient only when the ratio of conversion is close to unity.

Voltage Reference element forms the foundation of linear regulator since V_{DD} must be either equal or a multiple of reference voltage V_{REF} .

For good regulation, V_{REF} must be stable across V_{DD} variations. Voltage Sample element monitors V_{DD} and translates it into a level equal to the V_{REF} for a desired regulated voltage. Variations in V_{DD} cause feedback which changes V_{SAMPLE} to some value greater than or less than the V_{REF} . ΔV_{SAMPLE} causes comparator to drive series or shunt element which would respond appropriately to correct the output voltage change.

Besides the textbook classic series and shunt voltage regulator, there is also a unique case of linear (resistive) based power converter circuit worth mentioning, which is a reconfigurable switch to control an array of PVCs (Lee et al. 2016). By using low impedance switches and basic digital logic control, as shown in Fig. 11.9, high power conversion efficiency (>90%) is achieved to control PVC array since

there is essentially zero switching loss. This circuit works under the assumption that the total, stacked output voltage of PVC array is always sufficient to direct charge a rechargeable battery.

11.3.2 Switching Converter and Switched-Capacitor (SC) Power Converter in Energy Harvesting Application

As discussed in Chap. 10, switching converter involves three different electrical components i.e. switches S_N , inductor L_N , diode D_N , with the objective of converting a given supply voltage V_{IN} , to output voltage V_{OUT} . There are three basic configurations possible, as illustrated in Fig. 10.2 of previous chapter. Buck converter shown in Fig. 11.2a (Chan and Mok 2011), is suitable for high voltage energy sources (PVC and PEH) where $V_{OUT} < V_{IN}$, Figure 11.2b is a Boost converter shown in Fig. 11.2b (Man et al. 2008), is suitable for low voltage energy sources (TEG and MFC) where $V_{OUT} > V_{IN}$. Buck-boost converter Chew et al. (2013), shown in Fig. 11.2c is suitable for hybrid energy harvester (combination of both high and low voltage sources) where V_{OUT} can be larger than or less than V_{IN} . All output-input voltage relationship of these converters can be adjusted by changing the switching clock duty cycle. The advantage of switching converter is the high conversion power efficiency, which can be up to 90%, achievable across different conversion ratio. The disadvantage is the requirement of off-chip inductor, which is bulky and expensive. Fully integrated on-chip switching converter is a popular on-going research topic (Huang and Mok 2013a, b).

An alternative to using inductor is by shifting to the other reactive circuit element, i.e. capacitor. Switched-capacitor (SC) power converter is also known as charge pump. The main advantage is that fully integrated on-chip implementation is possible and bi-directionality of conversion. For applications where bulky off-chip components must be avoided, charge pump is a good compromise between linear

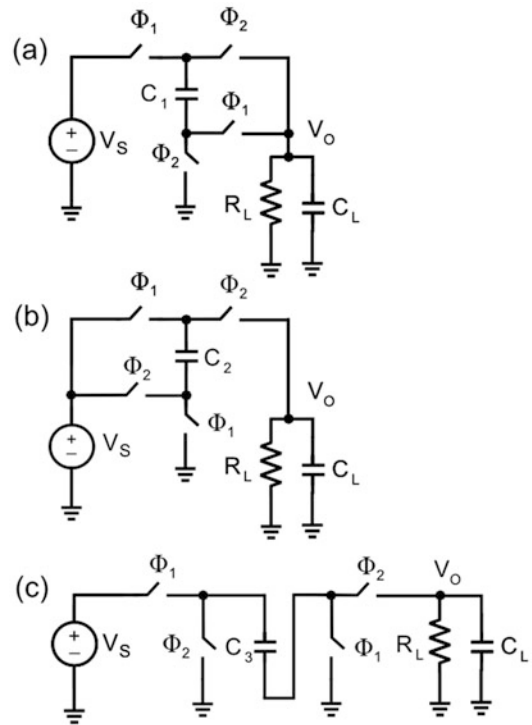


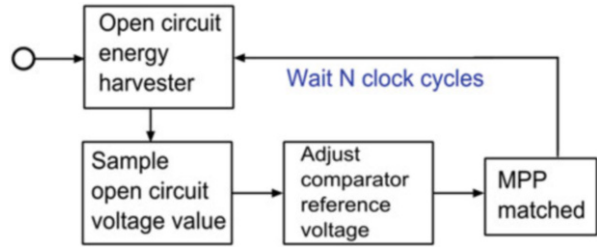
Fig. 11.10 Basic working principle of switched-capacitor DC-DC converter for (a) step-down, (b) step-up, (c) invert

regulator and switching. Similar to the switching counterpart, as shown in Fig. 11.10, there are three basic switched-capacitor configurations, which allow designers to step down (Jiang et al. 2014), step up (Su and Ki 2007) and invert (Wang and Wu 1997) a given voltage. Typically 50% duty 2-phase (Φ_1, Φ_2) clock is used. The invert charge pump is useful in generating negative voltage, which is instrumental in sub-threshold level power converter to suppress start-up system leakage (Kim et al. 2014).

11.3.3 Maximum Power Point Tracking in Energy Harvesting

Due to the volatile nature of energy harvesting source, it is important that the interfacing power management unit maximizes the charge extraction from the source, to minimize system down time before the loading IoT node is ready to

Fig. 11.11 Conventional maximum power point tracking algorithm



perform the next duty-cycled workload. The maximum power point is reached when the internal resistance of energy harvesting source is matched to the effective load connected. PVC often has non-linear peak output power point but TEG is linear, where the maximum power point is always half of the open-circuit voltage. A typical conventional maximum power point tracking (MPPT) algorithm for thermoelectric harvesting, as shown in Fig. 11.11 for a switching converter (Im et al. 2012) requires sampling of TEG open circuit voltage (V_{OC}), and then modifies the DC-DC converter duty cycle to change the input voltage to match the $0.5 V_{OC}$. This approach needs to periodically switch off converter so that V_{OC} can be sampled and updated according to environmental change. The alternative, perturb and observe (P&O) MPPT method is not commonly used in microwatts systems due to the high power consumption of voltage/current sensor.

Since internal resistance R_S is a known constant value with TEG, we can achieve continuous-time tracking of MPP by setting the input impedance to match R_S , without the need to sample V_{OC} . The associated algorithm is shown in Fig. 11.12. This idea effectively leverages on the advantage of a clock-power stage integrated boost converter reported in (Teh and Mok 2014a).

The input impedance of this boost converter can be derived from timing of the self-generating pulse. This assumption is valid as the temperature variation of R_S of thin-film TEG (Micropelt) is less than 1% of its nominal value, even when ΔT is up to 60 °C. However, since ΔT in typical energy harvesting application is small, such variance is acceptable and R_S can be regarded

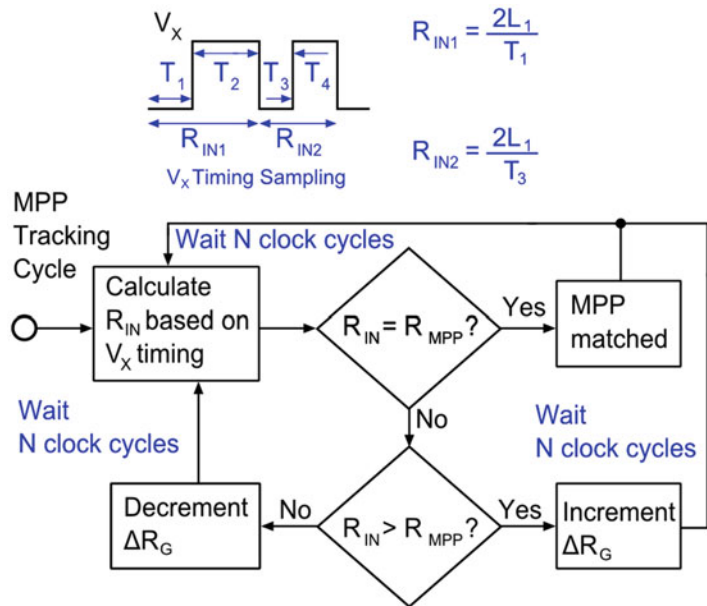
constant. To ensure absolute variability is less than 5%, simulations based on the assumption R_S varies by 20% (an excessive approximation), the tracked MPP voltage is only off by 5%. For very high performance system, designers need to incorporate additional temperature sensor and look-up table containing the temperature variation information R_S to compensate for all process, voltage and temperature (PVT) variation accurately. Since typical sampling pulse is of a few hundreds μs to ms range, digital clock can be run at MHz (100s of ns) clock range. The power consumption of such on-chip MPPT circuit is estimated to be within the ballpark of 100 μW when active. If MPPT algorithm is allowed to be run at low duty cycle (once for every few second, since temperature change is typically slow), average power can be reduced to microwatts range.

Another continuous-time MPPT method, as shown in Fig. 11.13, is to observe the output power via sampling the voltage accumulated over an on-chip capacitor. Within fixed clock period, the charge pump clock varies according to input voltage and hence the voltage-domain sensing is shifted to time-domain sensing, i.e. the higher power harvester is translated to shorter rising time. This approach effectively circumvents the power hungry voltage/current sensor problem (Liu et al. 2016).

11.3.4 Unique “Investment” Concept in Piezoelectric Harvesting

Kinetic energy in motion is attractive because vibrations are abundant in the environment. This is why piezoelectric transducers are popular today, and because they generate more power

Fig. 11.12 Continuous-time maximum power point tracking algorithm for switching topology based on (Teh and Mok 2014a)



Shorter Tr represents higher harvested power

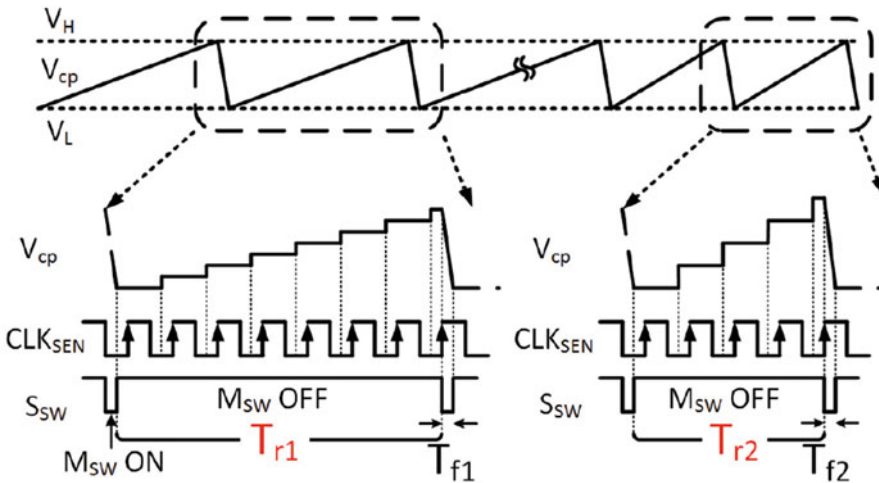


Fig. 11.13 Time-domain maximum power point tracking algorithm for switched-capacitor power converter based on (Liu et al. 2016)

from motion under similar space constraints than their electrostatic and electromagnetic counterparts. In piezoelectric harvesting, there is a unique harvesting technique that is not present in other energy harvesting modes which is the concept of investment. The idea is to strengthen the electrostatic force against which vibrations

work. This way, the circuit eventually draws dividend from the investment, i.e. extracting more power from the transducer after investing fixed amount of battery energy into PEH (Kwon and Rincon-Mora 2014). The operation waveforms of such piezoelectric harvesting mechanism are shown in Fig. 11.14.

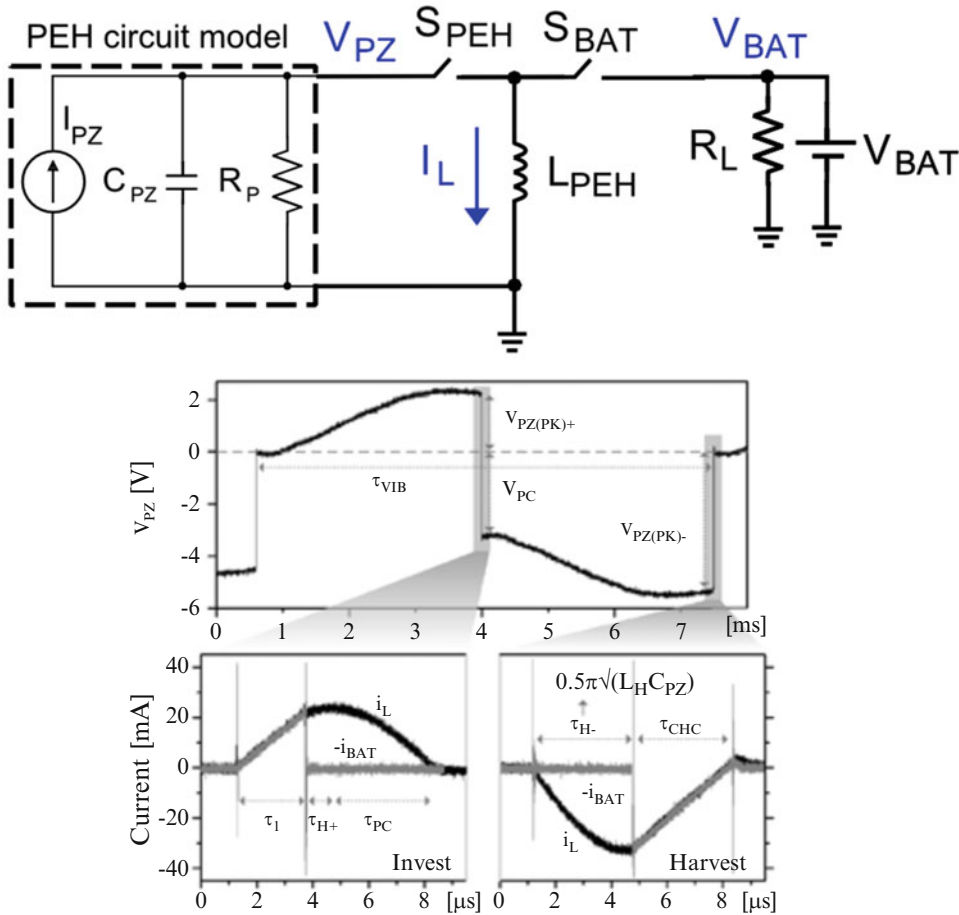


Fig. 11.14 Energy investing concept in piezoelectric harvesting (Kwon and Rincon-Mora 2014)

11.4 Adaptation to Source and Load

11.4.1 One-Shot Input Voltage in Piezoelectric Harvesting

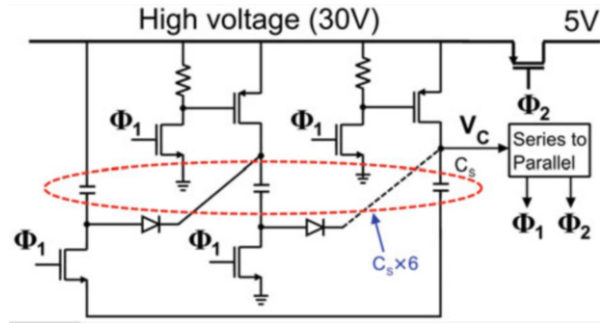
Typically, piezoelectric harvesters generate the most power when they vibrate at their resonant frequency. Unfortunately, motion is not always consistent or periodic. In many applications, in fact, vibrate in response to one-shot shocks, or repeated impact. Many related work such as (Kwon and Rincon-Mora 2014) discussed earlier can still function with one-shot or shocks but are not optimized for such operation mode. One interesting work (Yang et al. 2015a) is to use switched capacitor topology to absorb the high

excitation voltage during shock, and then, as shown in Fig. 11.15. The idea is to stack multiple capacitors in series during high voltage transient, and then redistribute the charge accumulated in parallel by reconfiguring the stacked capacitors, subsequently lowering the accumulated voltage.

11.4.2 Shunt Regulator as Protection Circuit

Under extreme low input stimulus as shown in Table 11.2, the output power from miniaturized PVC and PEH is of microwatts range, albeit output voltage at open circuit condition of these sources can be as high as 8 V. Considering the

Fig. 11.15 Series-parallel switched-capacitor to absorb high voltage overshoot (Yang et al. 2015a)



burst mode nature of incoming power, isolation diodes and interfacing power IC are especially vulnerable to breakdown. In standard CMOS 0.13- μm process, the nominal voltage is only 1.2 V for thin oxide transistor and 3.3 V for thick oxide transistor. Obviously input protection circuit needs to be included to avoid overvoltage breakdown caused by such high harvester output voltage. Conventionally series regulator such as low dropout regulator (LDO) is preferred over shunt regulator for higher power efficiency but this topology does not provide any input protection. When input voltage is as high as 8 V, the differential voltage across the dropout transistor is 5 V, if the output voltage is set to 3 V; this condition exceeds the drop out transistor breakdown limit. Shunt regulator is a straight forward solution to protect the load from the sudden voltage surge of the energy harvesting source and this cause reduction in power efficiency due to the constant quiescent power drawn by a shunt regulator.

To build a low quiescent shunt regulator, Schmitt-Trigger as shown in Fig. 11.16 can be deemed as the ideal candidate to optimize power consumption in this context (Teh and Mok 2014b). Conventional “problem” i.e. more gain for positive cycle and less gain for negative cycle is paradoxically again becomes favorable for shunt regulator application. Negative cycle of input voltage implies insufficient power from energy harvesting source; subsequently lowering gain of Schmitt-Trigger and cause more current to be diverted to the load instead of being shunted to ground via P_{SHUNT} . During positive cycle of input voltage (more harvested power), Schmitt-Trigger

has higher gain which helps shunting extra current to ground. In the default implementation, R_{COMP} represents the equivalent resistance of transistor drain-body junction leakage component. To further adjust the targeted output voltage after fabrication, the value of resistor R_{COMP} can be adjusted by having an additional bond pad to access the V_{SHUNT} node and connect an additional off-chip resistor. This off-chip resistor is only able to compensate for the process variation whenever R_{COMP} is higher than the simulated value. Note that this circuit is susceptible to CMOS process variation and can only offer coarse voltage regulation with 100 mV margin of error.

11.4.3 Multiple Input Multiple Output Voltage Requirements

Existing energy harvesting systems is commonly powered by single energy harvesting source with photovoltaic cell being the most popular and matured technology. Nevertheless a single source energy harvesting system is often intermittent and unpredictable in term of power generated. Instead of increasing storage capacitor or battery size, recent research direction is to pursue energy harvesting schemes using multiple energy sources. The key challenge is the design of interfacing power management circuit that efficiently combines many energy sources into common storage device. Combining the power from multiple time-varying sources typically requires a sophisticated control system.

A capacitor is analogous to storage reservoir for electrical charge carriers, as a water bucket to

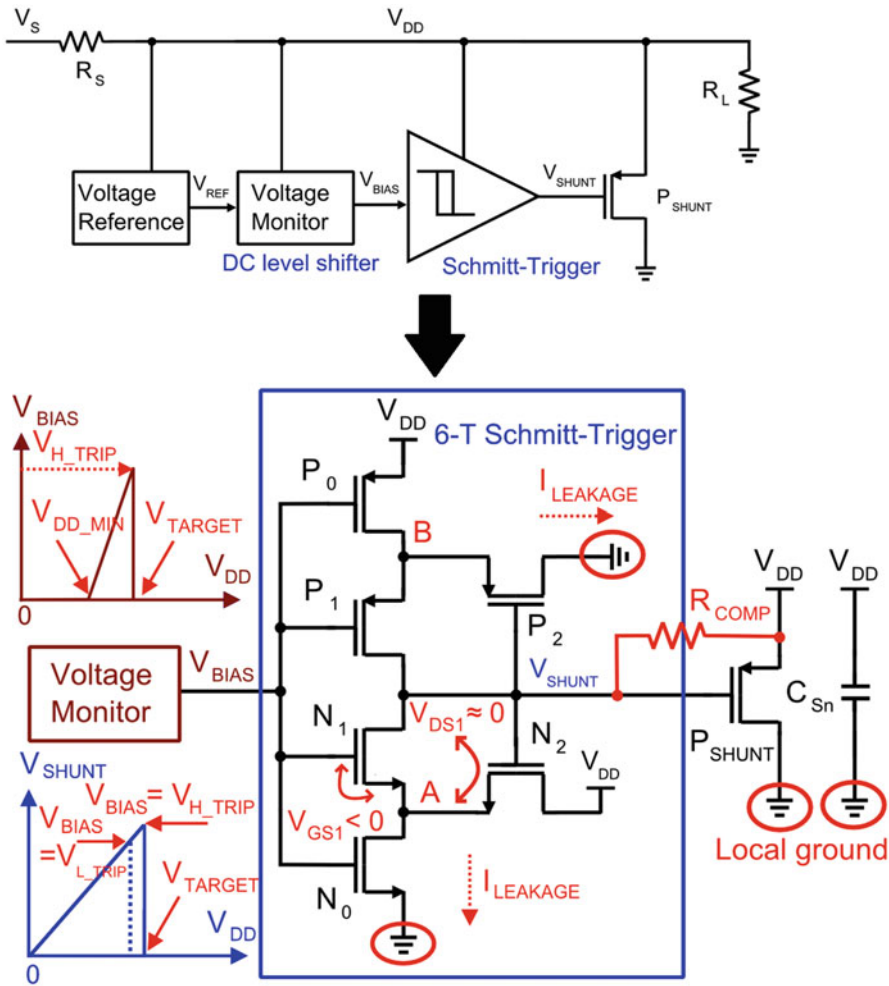


Fig. 11.16 Digital logic based implementation of shunt voltage regulator (Teh and Mok 2014b)

water flow. The capacitor leakage current can be compared to the water seeping through the water bucket. A capacitor will never become fully charged if the leakage current is greater than or equal to the supply current. Designer needs to take extra caution especially when these capacitors are to be charged by microwatts power source as the charging current are comparable to leakage current. Recently, molecularly thin film capacitor of 28 nm thickness (claimed to be better than graphene) and capacitance density of $27.5 \mu\text{F}/\text{cm}^2$, which is a factor of three orders better than commercial products in market, was fabricated using oxide nanosheets (Wang et al. 2014). Leakage current versus

applied voltage characteristics of such emerging capacitor type is shown in Fig. 11.17, of which leakage current is exponentially dependent on DC bias.

Connecting capacitors in series results in the voltage being split between the capacitors and in turn this is influenced by the leakage current difference between the individual capacitors in a series, as shown in Fig. 11.18. The leakage current component can be modeled as a parallel resistor to the capacitor. The leakage current differences become apparent when the circuits are activated in the form of overvoltage on the component with the lowest leakage current. Since considerable fluctuations are found

between individual capacitors (even from the very same production run) in terms of their leakage currents and capacitance, it is possible that large voltage differences may occur and one capacitor in the stacks will sustain higher voltage despite all having the same nominal capacitance. It is therefore important that both capacitance and leakage current differences are balanced in

the system since leakage current can vary up to two order of difference.

The simplest form of balancing circuit is a fixed value resistor parallel to each capacitor. However, this method merely provides balanced voltage but not voltage regulation. To obtain both balancing and regulated voltage, a low quiescent current shunt regulator (with minimal leakage current in its internal voltage reference and parasitic junction diodes) is a better candidate. A proposed scheme essentially emulates a water bucket fountain by envisioning capacitor as individual water bucket; as illustrated in Fig. 11.18 (Teh and Mok 2014b). Incoming charge from high voltage low current (HVLI) energy harvesting sources i.e. PVC and PEH will charge up stack capacitors directly. Once capacitor voltage reaches the set value, excess charge will be pushed to next capacitor below, and eventually to ground if all capacitors are fully charged to preset ΔV value i.e. 1 V. This operation is similar to push pull shunt regulation discussed in (Alon and Horowitz 2008). Diodes can be used to isolate incoming power of PVC and PEH.

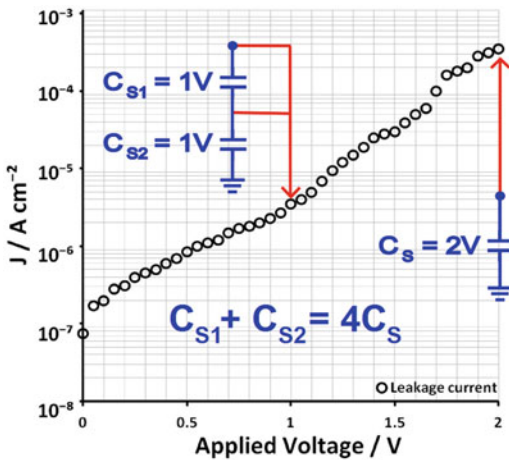


Fig. 11.17 Leakage current versus voltage profiles of the ultrathin capacitor (Wang et al. 2014)

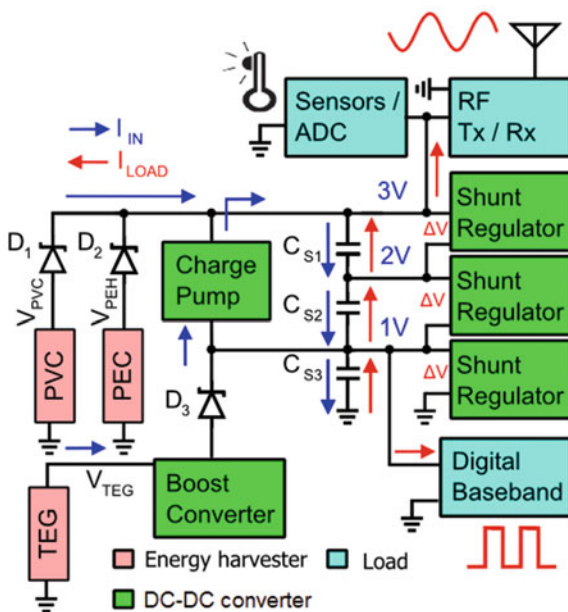


Fig. 11.18 Stacked capacitor energy harvesting scheme (Teh and Mok 2014b)

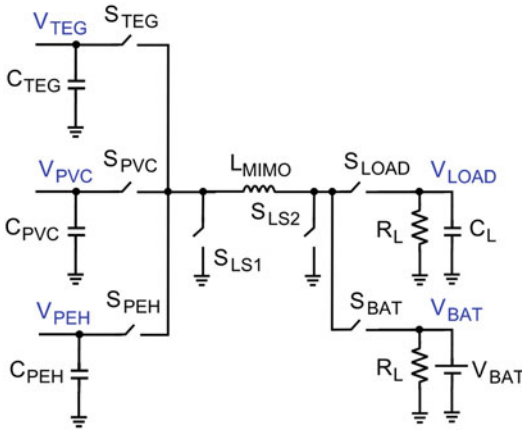


Fig. 11.19 Single-inductor multiple-input-multiple-output energy harvesting scheme (Bandyopadhyay and Chandrakasan 2012)

By combining the idea of divided series capacitor voltage to provide multiple voltage level, by connecting multiple capacitors in series, multiple voltage levels can be generated. Top capacitor (3 V) can power high voltage circuits (I/O, sensors, ADC, analog and RF) and bottom capacitor (1 V) can power low voltage low power digital circuits. In this proposed scheme, high incoming power can be driven directly by the primary power source when it is available. However when ambient power is insufficient, capacitor stacks will act as “flying-battery” configuration (Alon and Horowitz 2008) to supply high power, short interval required by IoT sensor node since each capacitor-shunt regulator pair forms a standalone “battery”. All capacitors in the stack therefore share a common DC current when IoT node draws current. Additional capacitor can be installed in parallel fashion if greater energy is demanded.

Besides the stacked capacitor approach, another popular research direction such as (Bandyopadhyay and Chandrakasan 2012) is to pursue energy harvesting schemes using multiple energy sources and simultaneously generate multiple output voltage, using single inductor as the core power conversion element, shown in Fig. 11.19. However, for such single inductor multi-input-multi-output topology, only one source can be polled at a time due to the implicit

time-multiplexing nature and the control is deemed complicated.

11.5 Voltage Limits and Cold Start

The caveat of employing the new generation, seemingly advantageous TEG is the increased R_{TEG} , which has lower output current. Such device characteristics put further design constraint, on top of the low voltage start-up operation, which is already a challenging task to solve. The main problem for a boost converter circuit to self-start-up is the limited voltage level generated by the TEG source, which is often below CMOS transistor’s threshold voltage (typically 300–500 mV). For body-wearable application with temperature difference of 1–2 °C, minimum output voltage can be as low as 25 mV. Therefore circuit designers face a catch-22 situation, where the dilemma is to bootstrap the boost converter in generating an output voltage of 1 V or more to power up other peripheral circuits such as sensors, analog-to-digital converter, digital baseband and RF transceiver. Since voltage up conversion always requires oscillation clock (which is generated on-chip or off-chip), as shown in Figs. 11.20 and 11.22. Therefore the solution to start-up problem fundamentally boils down to designing a sub-threshold oscillation clock generator at the lowest voltage possible. Many recent innovations in energy harvesting therefore focus on optimization of cold-start conditions in no-battery or dead-battery situations.

The minimum operation voltage of a binary switching signal transfer limit is known as the Meindl limit (Meindl and Davis 2000) where the theoretical minimum operation supply voltage (V_{DD}) is 36 mV (where 1’s and 0’s in signals are discernible) for ring oscillator implemented in standard CMOS technology. Another subtle start-up problem arises for systems employing TEG with high R_{TEG} , significant voltage drop across R_{TEG} and low current reduces transistor’s gm. This jeopardizes the feedback gain required by oscillators, which need relatively high current

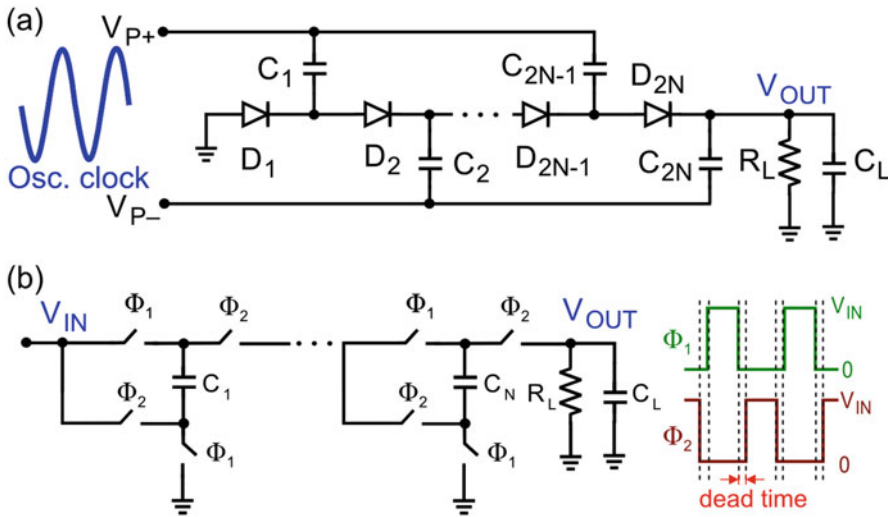


Fig. 11.20 (a) RF-pulse driven charge pump (b) On-chip clock driven charge pump

to function despite the low V_{DD} requirement (Teh and Mok 2014a).

To accomplish voltage boost conversion, linear regulator which is purely resistive is out of consideration since it can only perform voltage down conversion. Switching converter has the lowest start-up voltage (21 mV) and has the best power efficiency at the cost of bulky external inductor. To achieve the lowest start-up voltage, low threshold or zero threshold transistors should be used. However, power efficiency at higher output voltage will be lowered due to the transistor off-state leakage loss, which is inversely proportional to threshold voltage. From empirical data reported in recent works, CMOS 130 nm process seems to be the optimal choice of technology. Adopting more expensive CMOS process with smaller transistor size, renders diminishing return-over-cost for the sake of achieving lower start-up voltage or better power efficiency due to higher transistor leakage loss. In systems with negative supply voltage (Teh and Mok 2014b), transistor leakage loss can be reduced by applying negative gate voltage. However, larger magnitude of negative bias does not suppress leakage current further due to gate-induced-drain-leakage (GIDL) effect (Chatterjee et al. 2003). For example, the optimal

reverse bias for CMOS 130 nm process is approximately -0.3 V, as shown in Fig. 11.21.

The control circuit of the microwatts power single inductor switching converter is mainly digital-based, using an on-chip oscillator and counter controlled pulse width to achieve zero current switching (ZCS) as shown in Fig. 11.22. Oscillator generates a clock signal, with a particular frequency and duty cycle, which drives the low-side switch, SW_{LS} . The same clock signal is then delayed and used to generate pulses that drive the high-side switch SW_{HS} . The pulse width is controlled by digital counter value. Adaptive dead-time control is employed to minimized synchronization mismatch loss. The minimum start-up voltage of early low voltage TEG-powered switching converter is around 600 mV. However, the peak power efficiency is high, reaching 75% and lowest input voltage is 20 mV once activated (Carlson et al. 2010). Transformer-based switching converters using either high turns-ratio (Im et al. 2012) or unity turn-ratio pulse transformer (Teh and Mok 2014a) further reduce the start-up voltage down to 21 mV, due to minimal overhead control circuit required and the embedment of oscillator into the power stage. With an extra diode and output capacitor, (Teh and Mok 2014a) can be

Fig. 11.21 Off-state leakage current versus reverse bias voltage for CMOS 130 nm transistors

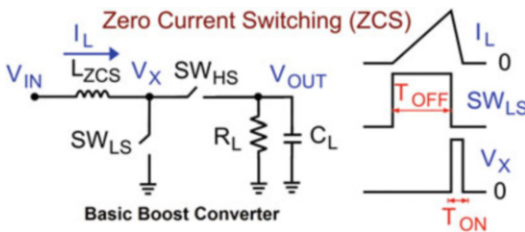
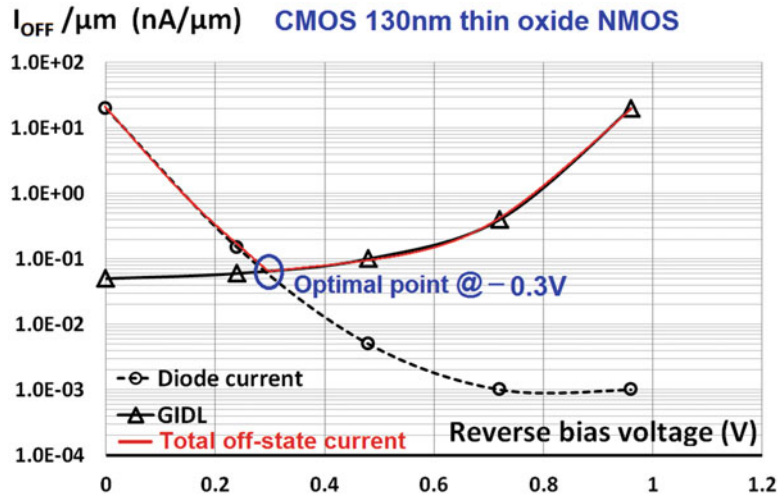


Fig. 11.22 Zero Current Switching (ZCS) control

reconfigured to give bipolar outputs up to ± 3 V (Teh and Mok 2014b).

Compared to the conventionally one-stage structure of switching converter, SC power converter usually comprises multiple passive diode-based or active gate driven stages due to the topology-constrained, finite voltage gain per stage, as shown in Fig. 11.20. Similar to switching converter, the minimum start-up of switched-capacitor power converter is bound by the minimal supply voltage required by its on-chip oscillation clock generation. By having more switches and sub-threshold gate drive voltage, SC power converter’s power efficiency at low voltage is lower than switching converter, especially for the fully integrated versions due to poor on-chip passives. Design techniques proposed to improve power efficiency of SC converter include adaptive dead-time control which alleviates shoot-through loss, negative voltage gate drive and substrate bias control to reduce

conductance loss (Kim et al. 2014). To eliminate the overhead of separate oscillator circuit, a self-oscillating SC converter is proposed (Jung et al. 2014). Hybrid converter refers to systems which employ both switching and SC converters in the system. LC-tank oscillator is used to generate sinusoidal clock (Bender Machado et al. 2014; Weng et al. 2013), which then drives a Dickson charge pump similar to those found in RFID tag RF-DC rectifier (Yi et al. 2009). (Fuketa et al. 2014) shows a fully integrated version using similar concept using on-chip transformers. Systems in (Chen et al. 2012b; Shrivastava et al. 2014) first self-starts using SC converter, which then drive another switching converter to provide the final output voltage. In (Bandyopadhyay et al. 2014), primary power converter is switching converter-based but SC converter is used to generate separate voltage to reduce high-side switch leakage. In (Teh et al. 2014), SC converter is used to supplement a SI converter, i.e. to transfer extra energy not consumed by the load to another secondary storage capacitor as backup.

Different self-start-up mechanisms reported in recent boost converter works are illustrated in Fig. 11.23. Performance of the representative papers of each start-up mechanism such as minimum start-up voltage, peak power efficiency and component requirements are summarized in Table 11.6. An interesting trend observed in research efforts to reduce start-up power is that

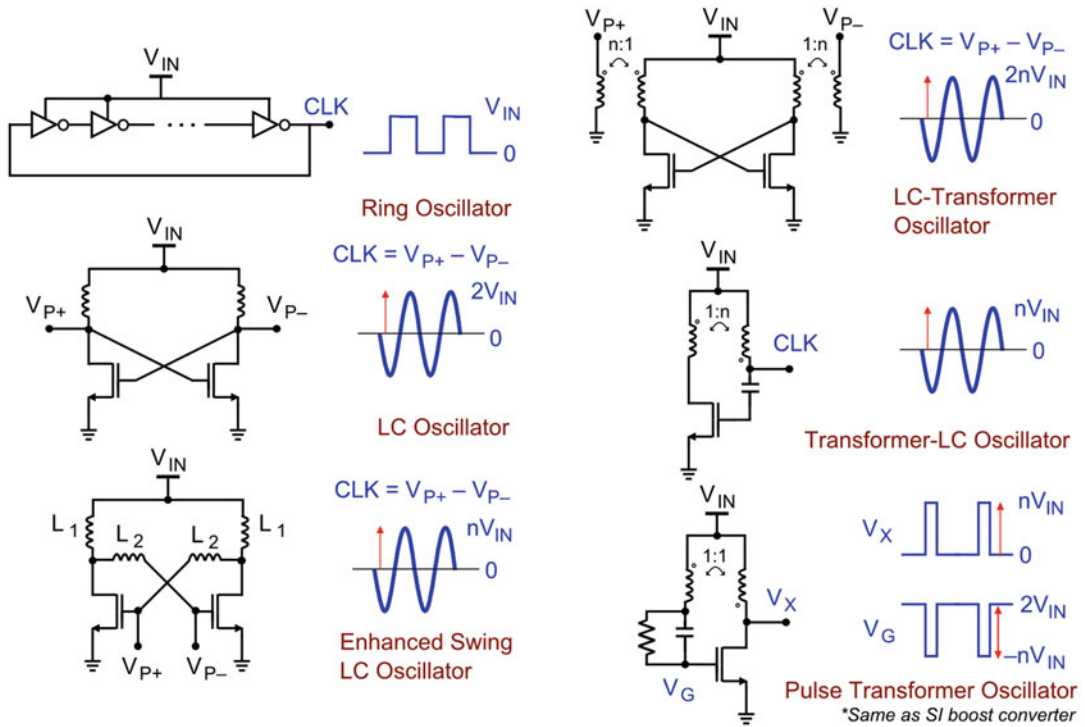


Fig. 11.23 Different self-start-up boost converter circuit topologies

Table 11.6 Performance summary of different topologies

Start-up mechanism & converter type	Performance			
	Min. start-up voltage	Peak power efficiency	External components	CMOS process
Ring oscillator	220 mV/ 70 mV	83%/58%	10 μ H inductor	130 nm
SC + Switching converter Shrivastava et al. (2014)/Goepfert et al. (2015)				
Ring oscillator	120 mV	39%	None	65 nm
SC converter Chen et al. (2012a)				
Ring oscillator	150 mV	73%	6×10 nF capacitors	130 nm
SC converter Kim et al. (2014)				
LC oscillator+Switching converter Weng et al. (2013)	50 mV	73%	2×2 μ H, 27 μ H, 100 μ H inductors	65 nm
Enhanced swing LC oscillator+SC converter Bender Machado et al. (2014)	10 mV	NA	2×9.5 μ H, 2×950 μ H inductors	130 nm
LC-transformer oscillator+SC converter Fuketa et al. (2014)	85 mV	1.5%	None	65 nm
Transformer-LC oscillator+Switching converter Im et al. (2012)	40 mV	61%	1:60 transformer	130 nm
Pulse transformer oscillator+Switching converter Teh and Mok (2014a)	21 mV	74%	1:1 transformer	130 nm

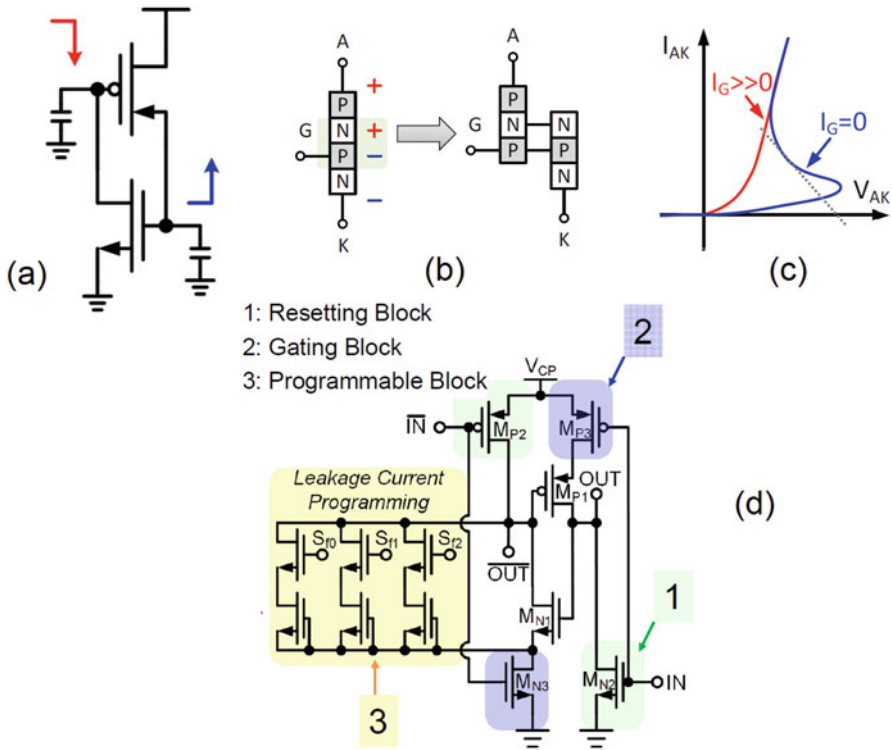


Fig. 11.24 (a) Leakage-based thyristor (b) Parasitic BJT to form equivalent thyristor (c) thyristor I-V curve (d) thyristor-based relaxation oscillator

non-conventional parasitic element in the CMOS process, such as a leakage based thyristor, using parasitic BJT junctions in the CMOS process, as shown in Fig. 11.24 is being used to design on-chip oscillator. The power consumption falls within the ballpark of sub-nanowatts (Liu et al. 2016). Ring oscillator based on a leakage-optimized Schmitt-Trigger cell shown in Fig. 11.25 is also proven the capability to start oscillating at only 70 mV supply voltage (Goepfert et al. 2015), without additional trimming as shown in (Chen et al. 2012b).

11.6 Passives in Energy Harvesting

Transformer-based systems often yield the best (lowest) self-start-up voltage performance, the inter-winding capacitance and series resistance

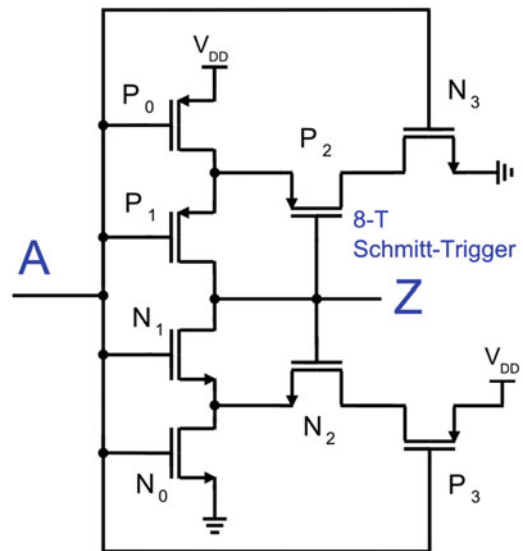


Fig. 11.25 Leakage-optimized Schmitt-Trigger cell (Goepfert et al. 2015)

Table 11.7 Electrical characteristics of high turns-ratio vs. unity turn-ratio transformer

Self-start-up boost converter topology	LC transformer oscillation	Pulse transformer oscillation
Transformer type	Non-standard, vendor specific Coilcraft LPR6235	Standard (Ethernet application) Murata 78601/9C
Turns-ratio	1:100	1:1
Coil resistance	316 Ω	1.3 Ω
Inter-winding capacitance	638 pF	121 pF
Inductance	7.5 μ H:75 mH	10 mH:10 mH
Coupling co-efficient (1.0 = perfect)	0.95	0.9999
PCB board space	6 \times 6 mm	9 \times 9 mm

of transformer coils are increased as transformer size is shrunk, as shown in Table 11.7. High turns-ratio transformer also has more flux leakage than pulse transformer besides the increased parasitic capacitance and resistance. On-chip transformer has lower quality factor (below 20) compared to off-chip inductors which is 80 or higher (Moazenzadeh et al. 2015). Another important external component is Schottky diode, where lower turn-on voltage and smaller junction capacitance is always desired. Besides, due to high voltage conversion ratio (high SI boost converter duty cycle), output capacitor is mostly in self-discharge state during the switching cycle, making capacitor leakage loss an important consideration. Capacitor with higher rated voltage should be used to reduce capacitor leakage loss which is exponentially dependent on biased voltage. Further miniaturization of the system size is yet another research direction. For instance, advanced three-dimension die stacking packaging technology (Yu et al. 2011) can further reduce system board area. Novel wire bonding techniques (Raimann et al. 2012) and new transformer material (Camarda et al. 2015; Raimann et al. 2012) to realize miniaturized transformer on PCB would also be interesting research topics to explore. On-chip capacitors are often associated with bottom plate parasitic that degrades the switched-capacitor power efficiency. However, the availability of deep trench capacitor has managed to push the power efficiency up to 90% levels (Jung et al. 2014).

11.7 Perspectives and Trends on Energy Harvested IoT Nodes

This chapter has presented a general overview of low power energy harvesting and the associated power management circuit techniques reported in the recent decade. Designers need to trade off the choice of circuit topology, external component and CMOS process, based on the application requirement i.e. minimal start-up voltage, power efficiency and system size. The time availability and power profile (determined by source resistance) of energy harvesting source used in the application also limits the choice of circuit topologies. Further innovation and major breakthrough will require first, the advancement of CMOS process with better leakage reduction and second, miniaturized integrated magnetic and capacitive components with higher density and quality factor.

The development of next generation energy harvesters and energy storage using flexible materials is an emerging research topic (Koo et al. 2012; Zhong et al. 2014). Despite enjoying the convenience of being wearable and bendable, these emerging devices also pose new design challenges for circuit designers, due to the interchangeable roles of energy storage and generators in operation, and also the fluctuating electrical characteristics. In recent years, 130 nm and 65 nm technology are commonly chosen for prototype implementation as both are considered

as optimum choice of CMOS technology for ultra-low voltage circuit design. Advanced CMOS technologies with shorter channel length have diminishing returns in advantages from the perspective of low voltage analog circuits (Galup-Montoro et al. 2012). However, it is still necessary to explore digital-based reprogrammable power management integrated circuits such as digital LDO (Yang et al. 2015b) which are capable of adapting to such unique device characteristics during in-circuit operation, especially under sub-1 V operations. Further study in designing an advanced reconfigurable charge pump topologies (Jung et al. 2014) which have multiple output, self-driven clock and balances bi-directionality of power flow would also be instrumental.

The control of multi-input-multi-output energy harvesting system typically requires additional overhead power, i.e. first sense the availability of power from each source, then compute and optimize the multi-source time multiplexing on the power converter. Similar to scarcity problem in wireless communication channel allocation, it is foreseen that game theoretic strategies and models can be employed to analyse harvested power supply and demand budget, and to optimize the converter utilization time allocation problem in a multi-source power converter. Hence a software-hardware co-design power management approach is foreseen to be the future trend of energy harvested IoT nodes.

References

- E. Alon, M. Horowitz, Integrated regulation for energy-efficient digital circuits. *IEEE J. Solid State Circuits* **43**(8), 1795–1807 (2008)
- S. Bandyopadhyay, A.P. Chandrakasan, Platform architecture for solar, thermal and vibration energy combining with MPPT and single inductor. *IEEE J. Solid State Circuits* **47**(9), 2199–2215 (2012)
- S. Bandyopadhyay, P.P. Mercier, A.C. Lysaght, K.M. Stankovic, A.P. Chandrakasan, A 1.1 nW energy harvesting system with 544pW quiescent power for next-generation implants, in *Proceedings of the IEEE International Solid State-Circuits Conference (ISSCC)* (2014), pp. 396–397
- M. Bender Machado, M. Sawan, M. Cherem Schneider, C. Galup-Montoro, 10 mV–1V step-up converter for energy harvesting applications, in *Proceedings of the Symposium on Integrated Circuits and Systems Design (SBCCI)* (2014), pp. 1–5.
- A. Camarda, A. Romani, E. Macrelli, M. Tartagni, A 32 mV/69 mV input voltage booster based on a piezoelectric transformer for energy harvesting applications. *Sensor. Actuat. A Phys.* **232**, 341–352 (2015)
- E.J. Carlson, K. Strunz, B.P. Otis, A 20mV input boost converter with efficient digital control for thermoelectric energy harvesting. *IEEE J. Solid State Circuits* **45**(4), 741–750 (2010)
- M.P. Chan, P.K.T. Mok, Design and implementation of fully integrated digitally controlled current-mode buck converter. *IEEE Trans. Circuits Syst. I* **58**(8), 1980–1991 (2011)
- B. Chatterjee, M. Sachdev, S. Hsu, R. Krishnamurthy, S. Borkar, Effectiveness and scaling trends of leakage control techniques for sub-130 nm CMOS technologies, in *Proceedings of the International Symposium on Low Power Electronics and Design (ISLPED)* (2003), pp. 122–127
- P.-H. Chen, K. Ishida, X. Zhang, Y. Okuma, Y. Ryu, M. Takamiya, T. Sakurai, A 120-mV input, fully integrated dual-mode charge pump in 65-nm CMOS for thermoelectric energy harvester, in *Asia and South Pacific Design Automation Conference (ASP-DAC)* (2012), pp. 469–470.
- P.-H. Chen, X. Zhang, K. Ishida, Y. Okuma, Y. Ryu, M. Takamiya, T. Sakurai, An 80 mV startup dual-mode boost converter by charge-pumped pulse generator and threshold voltage tuned oscillator with hot carrier injection. *IEEE J. Solid State Circuits* **47**(11), 2554–2562 (2012b)
- K.W.R. Chew, Z. Sun, H. Tang, L. Siek, A 400 nW single-inductor dual-input-tri-output DC-DC buck-boost converter with maximum power point tracking for indoor photovoltaic energy harvesting, in *IEEE International Solid-State Circuits Conference Digest of Technical Papers* (2013), pp. 68–69.
- M. Danesh, J.R. Long, An autonomous wireless sensor node incorporating a solar cell antenna for energy harvesting. *IEEE Trans. Microw. Theory Tech.* **59**(12), 3546–3555 (2011)
- Enocean, Solar Cells ECS300 and ECS310 [Online]. http://www.enocean.com/en/enocean_modules/ecs-300-data-sheet-pdf
- H. Fuketa, Y. Momiyama, A. Okamoto, T. Sakata, M. Takamiya, T. Sakurai, An 85-mV input, 50- μ s startup fully integrated voltage multiplier with passive clock boost using on-chip transformers for energy harvesting, in *Proceedings of the European Solid State Circuits Conference (ESSCIRC)* (2014), pp.263–266
- C. Galup-Montoro, M.C. Schneider, M.B. Machado, Ultra-low voltage operation of CMOS analog circuits:

- amplifiers, oscillators, and rectifiers. *IEEE Trans. Circuits Syst. II Exp. Briefs* **59**(12), 932–936 (2012)
- J. Goepfert, Y. Manoli, Inductive boost converter for thermoelectric energy harvesting with fully integrated start-up at 70 mV, in *Proceedings of the European Solid State Circuits Conference (ESSCIRC)* (2015), pp. 233–236.
- E.N.Y. Ho, P.K.T. Mok, Wide-loading-range fully integrated LDR with a power-supply ripple injection filter. *IEEE Trans. Circuits Syst. II* **59**(6), 356–360 (2012)
- C. Huang, P.K.T. Mok, A 100 MHz 82.4% efficiency package-bondwire based four-phase fully-integrated buck converter with flying capacitor for area reduction. *IEEE J. Solid State Circuits* **48**(12), 2977–2988 (2013a)
- C. Huang, P.K.T. Mok, An 84.7% efficiency 100-MHz package bondwire-based fully integrated buck converter with precise dcm operation and enhanced light-load efficiency. *IEEE J. Solid State Circuits* **48**(11), 2595–2607 (2013b)
- J.P. Im, S.W. Wang, S.T. Ryu, G.H. Cho, A 40 mV transformer-reuse self-start-up boost converter with mppt control for thermoelectric energy harvesting. *IEEE J. Solid State Circuits* **47**(12), 3055–3067 (2012)
- J. Jiang, Y. Lu, W.H. Ki, Analysis of two-phase on-chip step-down switched capacitor power converters, in *IEEE Asia Pacific Conference on Circuits and Systems (APCCAS)*, Ishigaki Island, Okinawa, Japan (2014), pp. 575–578
- X. Jing, P.K.T. Mok, Power loss and switching noise reduction techniques for single-inductor multiple-output regulator. *IEEE Trans. Circuits Syst. I* **60**(10), 2788–2798 (2013)
- W. Jung, S. Oh, S. Bang, Y. Lee, D. Sylvester, D. Blaauw, A 3nW fully integrated energy harvester based on self-oscillating switched-capacitor DC-DC converter, in *Proceedings of the IEEE International Solid State Circuits Conference (ISSCC)* (2014), pp. 398–399
- J. Kim, P.K.T. Mok, C. Kim, A 0.15V-input energy-harvesting charge pump with switching body biasing and adaptive dead-time for efficiency improvement, in *Proceedings of the IEEE International Solid State Circuits Conference (ISSCC)* (2014), pp. 394–395
- M. Koo, K. Park, S. Lee, M. Suh, D.Y. Jeon, J.W. Choi, K. Kang, K.J. Lee, Bendable inorganic thin-film battery for fully flexible electronic systems. *Nano Lett.* **12**(9), 4810–4816 (2012)
- D. Kwon, G.A. Rincon-Mora, A single-inductor 0.35- μm CMOS energy-investing piezoelectric harvester. *IEEE J. Solid State Circuits* **49**(10), 2277–2291 (2014)
- I. Lee, W. Lim, A. Teran, J. Philips, D. Sylvester, D. Blaauw, A $> 78\%$ efficient light harvester over 100-to-100klux with reconfigurable PV-cell network and MPPT circuit, in *IEEE International Solid-State Circuits Conference Digest of Technical Papers* (2016), pp. 370–372
- X. Liu, E. Sanchez-Sinencio, A single-cycle MPPT charge-pump energy harvester using a thyristor-based vco without storage capacitor, in *IEEE International Solid-State Circuits Conference Digest of Technical Papers* (2016), pp. 364–365
- D. Ma, W.H. Ki, C.Y. Tsui, P.K.T. Mok, Single-inductor multiple-output switching converters with time-multiplexing control in discontinuous conduction mode. *IEEE J. Solid State Circuits* **38**(1), 89–100 (2003a)
- D. Ma, W.H. Ki, C.Y. Tsui, A pseudo-CCM/DCM SIMO switching converter with freewheel switching. *IEEE J. Solid State Circuits* **38**(6), 1007–1014 (2003b)
- P.I. Mak, R.P. Martins, High-/mixed-voltage RF and analog CMOS circuits come of age. *IEEE Circuits Syst. Mag.* **10**(4), 27–39 (2010)
- T.Y. Man, P.K.T. Mok, M. Chan, A 0.9-V input discontinuous-conduction-mode boost converter with CMOS-control rectifier. *IEEE J. Solid State Circuits* **43**(9), 2036–2046 (2008)
- Marlow Industries, TG12-2.5 Datasheet [Online]. <http://www.marlow.com/media/marlow/product/downloads/tg12-2-5-011/TG12-2.5.pdf>
- J.D. Meindl, A.J. Davis, The fundamental limit on binary switching energy for terascale integration (TSI). *IEEE J. Solid State Circuits* **35**(10), 1515–1516 (2000)
- Microgen, MEMS-based vibrational energy harvesting [Online]. <http://www.microgensystems.com>
- Micropelt, MPG-D751 Datasheet [Online]. http://www.micropelt.com/down/datasheet_mpg_d651_d751.pdf
- A. Moazenzadeh, F.S. Sandoval, N. Spengler, V. Badilita, U. Wallrabe, 3-D Microtransformers for DC-DC on-chip power conversion. *IEEE Trans. Power Electron.* **30**(9), p5088 (2015)
- M. Raimann, A. Peter, D. Mager, U. Wallrabe, J.G. Korvink, Microtransformer-based isolated signal and power transmission. *IEEE Trans. Power Electron.* **27**(9), 3996–4004 (2012)
- P. Sarkar, S. Chakrabarty, Compressive self-powering of Piezo-floating-gate mechanical impact detectors. *IEEE Trans. Circuits Syst. Regul. Pap.* **60**(9), 2311–2320 (2013)
- A. Shrivastava, D. Wentzloff, B.H. Calhoun, A 10mV-input boost converter with inductor peak current control and zero detection for thermoelectric energy harvesting, in *Proceedings of the IEEE Custom Integrated Circuits Conference (CICC)* (2014), pp. 1–4
- F. Su, W.H. Ki, Design strategy for step-up charge pumps with variable integer conversion ratios. *IEEE Trans. Circuits Syst. II* **54**(5), 417–421 (2007)
- Y.K. Teh, P.K.T. Mok, Design of transformer-based boost converter for high internal resistance energy harvesting sources with 21 mV self-start-up voltage and 74% power efficiency. *IEEE J. Solid State Circuits* **49**(11), 2694–2704 (2014a)
- Y.K. Teh, P.K.T. Mok, A stacked capacitor multi-microwatts source energy harvesting scheme with

- 86 mV minimum input voltage and ± 3 V bipolar output voltage. *IEEE J. Emerging Sel. Top. Circuits Syst.* **4**(3), 313–323 (2014b)
- Y.K. Teh, P.K.T. Mok, A bipolar output voltage pulse transformer boost converter with charge pump assisted shunt regulator for thermoelectric energy harvesting, in *Proceedings of the IEEE Midwest Symposium on Circuits and Systems (MWSCAS)* (2014), pp. 37–40
- C.C. Wang, J.C. Wu, Efficiency improvement in charge pump circuits. *IEEE J. Solid State Circuits* **32**(6), 852–860 (1997)
- H. Wang, G. Wang, Y. Ling, F. Qian, Y. Song, X. Lu, S. Chen, Y. Tong, Y. Li, High power density microbial fuel cell with flexible 3D graphene-nickle foam as anode. *Nanoscale* **5**(21), 10283–10290 (2013)
- C. Wang, M. Osada, Y. Ebina, B.-W. Li, K. Akatsuka, K. Fukuda, W. Sugimoto, R. Ma, T. Sasaki, All-nanosheet ultrathin capacitors assembled layer-by-layer via solution-based processes. *ACS Nano* **8**(3), 2658–2666 (2014). doi:[10.1021/nn406367p](https://doi.org/10.1021/nn406367p)
- P.S. Weng, H.Y. Tang, P.C. Ku, L.H. Lu, 50 mV-input batteryless boost converter for thermal energy harvesting. *IEEE J. Solid State Circuits* **48**(4), 333–341 (2013)
- J. Yang, M. Lee, M.J. Park, S.Y. Jung, J. Kim, A 2.5-V, 160- μ J-output piezoelectric energy harvester and power management IC for Batteryless Wireless Switch (BWS) applications, in *2015 Symposium on VLSI Circuits Digest of Technical Papers* (2015), pp. 282–283
- F. Yang, P.K.T. Mok, A 0.6-1V input capacitor-less asynchronous digital LDO with fast transient response achieving 9.5b over 500mA loading range in 65-nm CMOS, in *European Solid State Circuits Conference (ESSCIRC)*, Graz, Austria (2015), pp. 180–183
- J. Yi, W.H. Ki, P.K.T. Mok, C.Y. Tsui, Dual-power-path RF-DC multi-output power management unit for RFID tags, in *Proceedings of the IEEE Symposium on VLSI Circuits (VLSIC)* (2009), pp. 200–201
- A. Yu, J.H. Lau, S.W. Ho, A. Kumar, W.Y. Hnin, W.S. Lee, M.C. Jong, V.N. Sekhar, V. Kripesh, D. Pinjala, S. Chen, C.-F. Chan, C.-C. Chao, C.-H. Chiu, C.-M. Huang, C. Chen, Fabrication of high aspect ratio TSV and assembly with fine-pitch low-cost solder microbump for Si interposer technology with high-density interconnects. *IEEE Trans. Compon. Packag. Manuf. Technol.* **1**(9), 1336–1344 (2011)
- C. Zhan, W.H. Ki, An output-capacitor-free adaptively biased low-dropout regulator with subthreshold undershoot-reduction for SoC. *IEEE Trans. Circuits Syst. I* **59**(5), 1119–1131 (2012)
- C. Zhan, W.H. Ki, Analysis and design of output-capacitor-free low-dropout regulators with low quiescent current and high power supply rejection. *IEEE Trans. Circuits Syst. I* **61**(2), 625–636 (2014)
- J. Zhong, Y. Zhang, Q. Zhong, Q. Hu, B. Hu, Z.L. Wang, J. Zhou, Fiber-based generator for wearable electronics and mobile medication. *ACS Nano* **8**(6), 6273–6280 (2014). doi:[10.1021/nn501732z](https://doi.org/10.1021/nn501732z)